Reference: *Biol. Bull.* **233:** 39–57. (August 2017)

Radiolar Eyes of Serpulid Worms (Annelida, Serpulidae): Structures, Function, and Phototransduction

MICHAEL J. BOK[1,*], MEGAN L. PORTER[2], HARRY A. TEN HOVE[3], RICHARD SMITH[4,†], AND DAN-ERIC NILSSON[1]

[1]*Lund Vision Group, Department of Biology, Lund University, Sölvegatan 35, 22362 Lund, Sweden;*
[2]*Department of Biology, University of Hawai'i at Mānoa, Honolulu, Hawai'i 96822;*
[3]*Naturalis Biodiversity Center, P.O. Box 9517, 2300 RA Leiden, The Netherlands;*
and [4]*Department of Marine Biology, James Cook University, Townsville, Queensland 4811, Australia*

Abstract. Fan worms, represented by sabellid and serpulid polychaetes, have an astonishing array of unusual eyes and photoreceptors located on their eponymous feeding appendages. Here we organize the previous descriptions of these eyes in serpulids and report new anatomical, molecular, and physiological data regarding their structure, function, and evolution and the likely identity of their phototransduction machinery. We report that, as in sabellids, serpulids display a broad diversity of radiolar eye arrangements and ocellar structures. Furthermore, the visual pigment expressed in the eyes of *Spirobranchus corniculatus*, a species of the charismatic Christmas tree worms, absorbs light maximally at 464 nm in wavelength. This visual pigment closely matches the spectrum of downwelling irradiance in shallow coral reef habitats and lends support to the hypothesis that these radiolar photoreceptors function as a silhouette-detecting "burglar alarm" that triggers a rapid withdrawal response when the worm is threatened by potential predators. Finally, we report on the transcriptomic sequencing results for the radiolar eyes of *S. corniculatus*, which express invertebrate c-type opsins in their ciliary radiolar photoreceptors, closely related to the opsin found in the radiolar eyes of the sabellid *Acromegalomma interruptum*. We explore the potential for a shared evolutionary lineage between the radiolar photoreceptors of serpulids and sabellids and consider these unique innovations in the broader context of metazoan eye evolution.

Received 28 April 2017; Accepted 5 September 2017; Published online 30 October 2017.

* To whom correspondence should be addressed. Present address: School of Biological Sciences, University of Bristol, Bristol BS8 1TH, United Kingdom. E-mail: mikebok@gmail.com.

† Present address: Blue Planet Productions, 6 Melbourne Street, Fairlight 2094, Australia.

Abbreviations: MSP, microspectrophotometry; PIA, phylogenetically informed annotation; TEM, transmission electron microscopy.

Online enhancements: supplemental table.

Introduction

Serpulids

The unusual radiolar eyes of fan worms are compelling subjects for improving our understanding of eye evolution, the emergence of new sensory systems and behaviors, and signal processing in distributed visual systems. We have previously examined the diversity of these eyes in the Sabellidae (Bok and Nilsson, 2016; Bok *et al.*, 2016), and we now turn to the Serpulidae. Serpulids are sessile polychaetes that alongside the sabellids and fabriciids (which lack radiolar eyes) comprise the fan worms within the clade Sabellida. Serpulids live within self-secreted calcified tubes out of which they project an anterior radiolar (or branchial) crown up into the water column. This radiolar crown is bilobed and likely derived from prostomial tissue homologous to the palps of other polychaetes (Orrhage, 1980; Orrhage and Müller, 2005). Each lobe of the crown consists of a number of heavily ciliated radioles that filter food particles out of the water, passing them down to the mouth, and that contribute to respiration.

When startled, fan worms rapidly withdraw into their fortified tubes in order to safeguard their radioles from grazing pred-

ators (Rullier, 1948; Nicol, 1950). The withdrawal response is extremely rapid and can be initiated by mechanical (DeVantier *et al.*, 1986; Pezner *et al.*, 2017) or visual (Nicol, 1950; Smith, 1985) stimulation, which is communicated down the radiolar nerves to the brain and on to the segmental musculature *via* giant axons (Nicol, 1948). As an additional line of defense, and in contrast with sabellids, most serpulids modify a single radiole into a peduncle topped by an enlarged operculum, a plug with a chitinous or calcareous endplate, that stoppers the tube opening when withdrawn.

There are currently 73 recognized genera of serpulids comprising over 500 species (ten Hove and Kupriyanova, 2009; WoRMS, 2017). However, despite numerous efforts at resolving the phylogeny of the family, serpulid taxonomy is still quite confusing (Kupriyanova *et al.*, 2006; Kupriyanova and Rouse, 2008; Kupriyanova and Nishi, 2010; Prentiss *et al.*, 2014). Some examples of practical difficulties are given in Ben-Eliahu and ten Hove (2011; notably for *Protula*, *Salmacina*, *Serpula*, *Spirobranchus tetraceros* (Schmarda, 1861), and *Vermiliopsis*). Although most (sub)clades of the serpulids seem reasonably well supported and constant in mentioned papers, the affiliation of the nominal subfamily Spirorbinae and that of *Salmacina*/*Filograna* in Lehrke *et al.* (2007) and Kupriyanova and Rouse (2008) is distinctly different from that in Prentiss *et al.* (2014), admittedly based on not entirely comparable data sets. Remarkably, the former family "Sabellidae" was found to be paraphyletic, necessitating the elevation of the sabellid subfamily Fabriciinae to full family rank (Kupriyanova and Rouse, 2008; Capa *et al.*, 2011). The three families, however, are well defined as a clade *versus* the outgroup genera.

Photoreceptors and eyes in serpulids

For the purposes of this report, we define ocelli and eyes as follows (after Bok *et al.*, 2016). Photoreceptors are the fundamental light-sensitive component of a visual system. When used in visual tasks beyond slow-integrating radiance detection, these sensory cells are identifiable by extensive membranous elaborations packed with light-transducing visual pigments that increase sensitivity. When photoreceptors produce, or are coupled with, directionality-conferring screening pigments, we term the resulting structure an ocellus, the simplest configuration of an "eye." From here, evolutionary processes can add optical units to improve light capture. Furthermore, multiple ocelli can be grouped together into a compound eye, or, alternatively, multiple photoreceptors can be pooled behind a shared aperture or lens, producing a simple eye. Both of these strategies can be elaborated to accommodate higher-order visual tasks based upon image-forming vision (for reviews see Nilsson, 2009, 2013).

Polychaetes have a surprising abundance of photoreceptors, ocelli, or eyes distributed across their bodies (Purschke, 2005; Purschke *et al.*, 2006). In general, these can be broadly grouped into four categories: cerebral, segmental, pygidial, and radiolar. Cerebral ocelli are defined here as being located in close association with the brain, within the peristomium or prostomium (excluding the radioles). They are present through development (Smith, 1984a, 1985), lost or reduced in many sedentary species, and elaborated into image-forming simple eyes in errant species such as *Platynereis dumerilii* (Audouin & Milne Edwards, 1834) (see Fischer, 1963) and most spectacularly in the alciopids (Wald and Rayport, 1977). Unlike sabellid fan worms, which often have well-developed segmental and pygidial ocelli (Ermak and Eakin, 1976; Dragesco-Kernéis, 1980), serpulid fan worms appear to be largely devoid of superficially obvious ocelli or eyes posterior to the collar. Notable exceptions include the genus *Placostegus*, which possibly has a belt of thoracic eyespots (ten Hove and Kupriyanova, 2009), and *Spirobranchus nigranucha*, which may have segmental eyespots on the abdomen (Smith, 1985, as *Spirobranchus* sp. D). Otherwise, adult serpulids typically have only simple clusters of cerebral ocelli at the base of the prostomium, closely associated with the brain. These cerebral ocelli are typically buried under obfuscating epithelial tissue and, furthermore, are often positioned below the rim of the animal's tube (Fig. 1A; Smith, 1985). Therefore, in order to avoid predation, many serpulids instead rely on radiolar eyes located on their feeding tentacles or the operculum. The radiolar eyes of fan worms were first noted in early taxonomic and anatomical works by Grube (1878), Andrews (1891), and Hesse (1899). In the 20th century, the radiolar eyes of serpulids have been mostly ignored in part due to a perceived lack of utility as a taxonomic character, especially in preserved material (Ben-Eliahu and ten Hove, 2011). However, some effort has been made to record observations regarding their presence and nature in fresh tissue (Smith, 1985; Table S1, available online).

Like sabellids (Lawrence and Krasne, 1965; Ermak and Eakin, 1976), the cerebral ocellar photoreceptors of serpulids are rhabdomeric in nature, with the elaborated photoreceptive membranes being formed from microvilli that project into a pigment cup (Figs. 1B, A1; Smith, 1984b). In contrast, the radiolar ocellar photoreceptors are ciliary, with the photoreceptive membrane being produced by stacked lamellae emerging from cilia (Fig. 1C; Smith, 1985). The radiolar ocelli are derived from epithelial cells in the outer aboral corners of the radioles (Fig. 1D), projecting their basal processes to the radiolar nerve and onto the branchial lobe of the brain.

Here we attempt to categorize the known diversity of radiolar ocelli in the Serpulidae as reported in previous anatomical and taxonomic investigations. We describe and compare new data on the fine structure of these ocelli from six serpulid species as revealed by transmission electron microscopy (TEM). Additionally, we report on phototransduction cascade components recovered from transcriptomic sequencing of the radiolar eyes of the Christmas tree worm *Spirobranchus corniculatus* (Grube, 1862). Finally, we report on

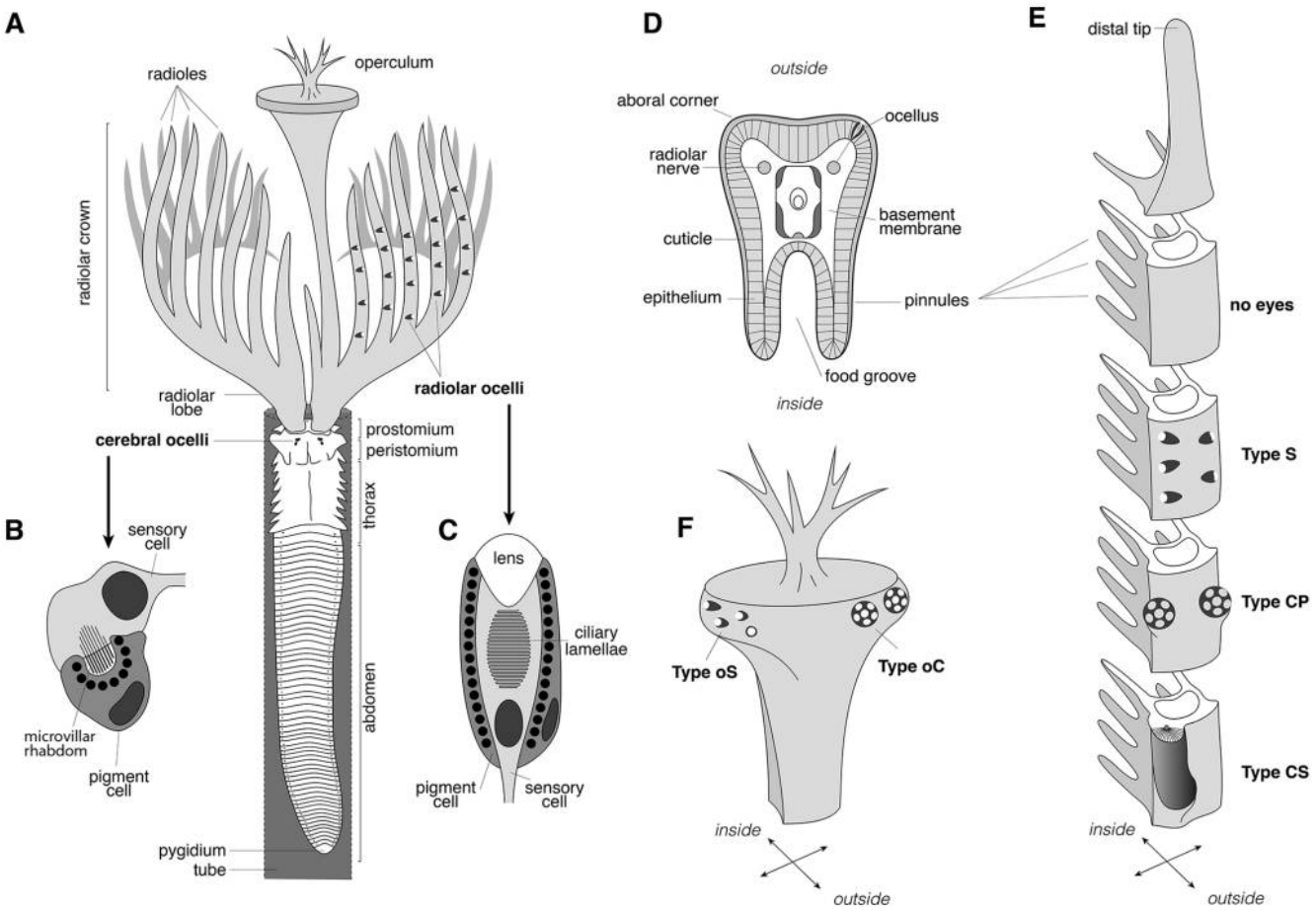

Figure 1. Ocelli and eyes in serpulids. (A) A generalized diagram of a serpulid; inset (B) with a simple diagram of a cerebral ocellus composed of a pigment cell and a rhabdomeric sensory cell that projects microvilli into the pigment cup; as well as a generalized diagram of (C) a radiolar ocellus including a pigment cup, formed by one or more pigment cells, a ciliary sensory cell that projects lamellar stacks into a sensory cavity, and a lens. (D) A diagram of a radiole in transverse section detailing relevant structures. (E) A diagram of a radiole with different configurations of radiolar eyes. (F) A diagram of the distal end of the operculum, detailing the two configurations of opercular, radiolar eyes. Radiolar and opercular eye types: CP, compound-paired; CS, compound-single; oC, opercular-compound; oS, opercular-simple; S, simple ocelli.

the spectral absorbance properties of the *S. corniculatus* photoreceptors, as revealed by microspectrophotometry (MSP). We discuss the evolutionary and functional implications of these results among serpulids, in contrast with sabellids, and in the grander context of the evolution of visual systems.

Materials and Methods

Animals

Serpulids displayed in this study were captured live at field stations: Carrie Bow Cay Field Station, Belize (administered by the Smithsonian Institution), September 2014 (*Pomatostegus stellatus*); Lizard Island Research Station, Queensland, Australia (administered by the Australian Museum, permit nos. SR-14-2004, SR-14-2003, SR-14-2005, SR-23-2009), March 2014 (*Spirobranchus corniculatus*); Estación de Investigación Costera (administered by the Mediterranean Institute for Advanced Studies [IMEDEA], collection permit from the Government of the Balearic Islands Ministry of Environment, Agriculture, and Fisheries), Mallorca, Spain, February 2016 (*Vermiliopsis* sp., *Serpula* sp., *Protula* sp.; shown in Fig. 2B–E). Additional materials were examined in the field by Harry ten Hove (see Table S1, available online, for details). *Spirobranchus* individuals for MSP were purchased at the live-fish store House of Tropicals in Baltimore, Maryland. The *Protula* sp. (Fig. 2A) was purchased from the live-fish store Bioted Marine in Kungsbacka, Sweden. All species used in electron microscopy besides *Pomatostegus stellatus* were wild captured by Richard Smith at a number of sites in temperate and tropical waters along the east coast of Australia. See Smith (1985) for complete details.

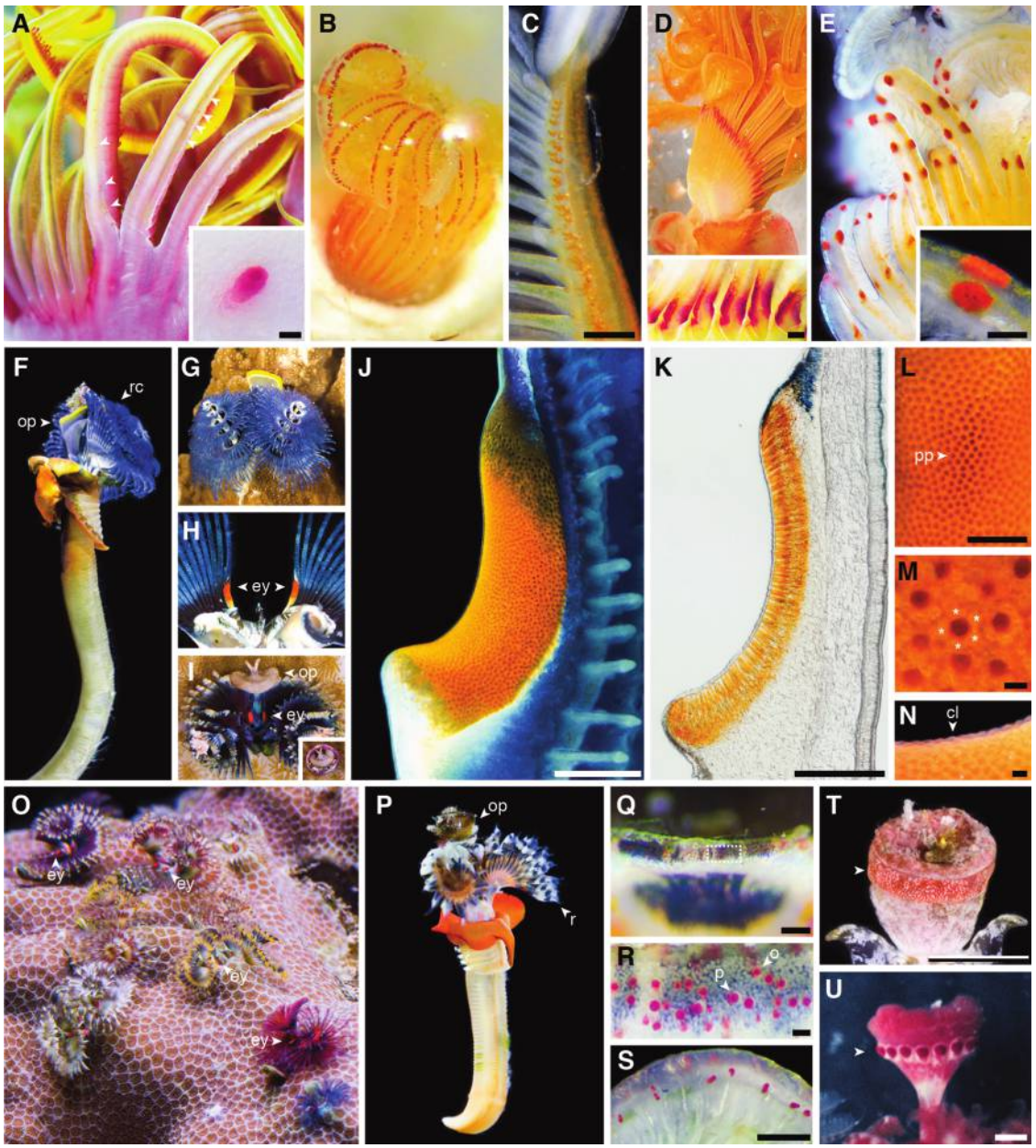

Figure 2. Radiolar eye arrangements in serpulids. (A) *Protula* sp. with minute type S ocelli along the radioles (arrowheads, inset). (B) An unidentified serpulid with densely packed, scattered type S ocelli all along both outer corners of the radioles. (C) The distal radiole of *Vermiliopsis* sp. with scattered type S ocelli. (D) *Serpula* sp. with a paired ocellar clusters near the base of each radiole (inset: magnified view of fixed tissue). (E) *Protula* sp. with type CP paired compound ocellar clusters (inset: magnified view of fixed tissue). (F–N) *Spirobranchus corniculatus*. (F) Adult removed from tube, with operculum (op) and radiolar crown (rc) indicated. (G) Adult, extended from tube, with eyes shielded from view by crown. (H) Crown with spires and operculum dissected away, revealing the eyes (ey). (I) Adult individual emerging from tube with radioles bunched, displaying eyes. (J) Close-up of *S. corniculatus* type S radiolar eye. (K) 14-μm-cryosection of *S. corniculatus* eye. (L) Micrograph of *S. corniculatus* eye showing a diffuse pseudopupil (pp). (M) *S. corniculatus* ocellar facets with the five pigment cells surrounding the sensory cavity indicated (asterisk). (N) A side view of *S. corniculatus* eye showing the cuticular lens facets (cl). (O) Several early-adult *Spirobranchus* individuals extended from their tubes with radiolar eyes visible. (P) *Pomatostegus stellatus* removed from tube, with operculum (op) and radioles (r) indicated. (Q) *P. stellatus* operculum with many type oS ocelli on the opercular brim. Dashed box indicates magnified view in (R). (R) Magnified view of *P. stellatus* opercular ocelli. Small orange (o) and large purple (p) types are visible. (S) *P. stellatus* radiole with similar ocelli to those seen on the operculum. (T) *Spirobranchus corrugatus* operculum with type oS ocelli along brim. (U) *Pyrgopolon* type oC opercular eyes. Photos: A–S, M. J. Bok; T, A. Semenov; U, H. A. ten Hove. Scale bars: (A inset), 10 μm; (C, D inset, E inset, L, S) = 100 μm; (J, K) = 200 μm; (N) = 20 μm; (M) = 10 μm; (Q) = 300 μm; (R) = 10 μm; (T, U) = 1 mm.

Photographs

Photographs of live animals displayed in Figure 2 were taken with a Canon T2i DSLR and a Canon EF 100mm f/2.8L Macro IS USM lens (Canon, Melville, NY). Raw photos were post processed for brightness, contrast, and color balance using Adobe Lightroom 5 photo editing software (Adobe Systems, San Jose, CA). Light photomicroscopy on fixed material was carried out using a Nikon (SMZ25; Minato, Tokyo, Japan) stereomicroscope with the SHR Plan Apo 2× objective. Images were captured using NIS-Elements software (Nikon). Fresh material was usually photographed on compound microscopes using 20× objectives with illumination from above both sides of the samples at roughly 45°. Images were captured using a Canon T2i DSLR with a microscope ocular adaptor lens. Focal series were captured through the depth of the radiole, and they assembled into a focus-stacked image using Zerene Stacker software (Zerene Systems, Richland, WA).

Transmission electron microscopy

For *P. stellatus*, tissue was fixed in the field in 2% paraformaldehyde (PFA), 2.5% glutaraldehyde, 2% sucrose in 0.1 mol l^{-1} Sörensen's phosphate buffer, pH 7.2, for 1 h at room temperature or overnight a 4 °C and was then stored in 0.1 mol l^{-1} Sörensen's phosphate buffer for transport to the lab. Individual radioles were washed in phosphate buffer (0.1 mol l^{-1}) followed by 1% osmium tetroxide in phosphate buffer for 1 h at 4 °C. Samples were washed in phosphate buffer, dehydrated on an ethanol series, infiltrated with acetone and Epon plastic (Electron Microscopy Sciences, Hatfield, PA), and embedded in Epon. Ultra-thin TEM sections (50–70 nm) were produced using a Leica (Wetzlar, Germany) Ultracut with a diamond knife and stained with 2% uranyl acetate and lead citrate (Reynolds, 1963). Sections were viewed on a JEM-1230 TEM (JEOL, Glen Ellyn, IL).

For all other species presented, refer to Smith (1985) for extensive detail. In brief, tissue was fixed in 1% osmium tetroxide in 0.1 mol l^{-1} sodium cacodylate buffer at pH 7.2–7.4 for 0.5–2 h at 4 °C or ambient temperature, followed by rinsing in the same buffer. The tissue was dehydrated on an ethanol series and infiltrated and embedded in Spurr resin. Sections were cut (90–30 nm) with a diamond knife (GeFeRi, Frosinone, Italy) and collected on copper grids. Sections were stained with uranyl acetate in acidified 50% ethanol followed by Reynold's modified lead citrate. Thin sections were visualized on Philips 300, Siemens Elmiskop 102, and Philips 400 electron microscopes operating at 60, 80, and 100 kV, respectively (Philips, Amsterdam; Siemens, Munich).

Microspectrophotometry

Visual pigment difference spectra were obtained from 14-μm transverse cryosections of *Spirobranchus corniculatus* radiolar eyes based on methods described previously (Cronin, 1985; Cronin and Marshall, 1989; Bok *et al.*, 2014). The animals were dark adapted for 48 h, and the eyes were dissected and sectioned under dim red illumination. The sections were mounted between coverslips in crustacean Ringer's solution (Cavanaugh, 1956). Photobleaching was performed with maximum transmitted illumination from the tungsten source between 3 and 7 min. Pre- and post-bleach absorbance measurements were subtracted in order to obtain the difference spectra, which were fitted using the A1 visual pigment template described in Stavenga *et al.* (1993). Absorbance of the photostable orange screening pigment was also measured.

Transcriptomics

Total RNA was extracted from the pooled radiolar eyes of six *S. corniculatus* individuals collected at Lizard Island Research Station using the Nucleospin RNA XS kit (Machery-Nagel, Düren, Germany) and quantified using a Qubit Fluorometer (ThermoFisher Scientific, Waltham, MA). Library construction and MiSeq (Illumina, San Diego, CA) sequencing of 300-bp paired-end reads was done by Molecular Research LP (Shallowater, TX), resulting in 10 million reads accessioned as BioSample SAMN0754970 in National Center for Biotechnology Information (NCBI) Bioproject PRJNA399760. Raw reads were quality checked and *de novo* assembled using the DNAStar software (Madison, WI) package. The resulting data set included 4.73 million reads, assembled into 8668 contigs with an average coverage of 9× and an N50 of 1540 bp. Phototransduction genes in the assembly were identified using phylogenetically informed annotation (PIA) by identifying query contigs phylogenetically placed close to landmark sequences with known functions; query contigs with long branches were not included (Speiser *et al.*, 2014). The identities of putative phototransduction-related transcripts identified from PIA were confirmed using reciprocal BLAST searches. Expression levels were calculated as fragments per kilobase million (FPKM) using read mapping in BowTie2, version 2.2.3 (Langmead and Salzberg, 2012), run on the National Center for Genome Analysis Support (NCGAS) Mason Linux Server (Indiana University, Bloomington, IN). Opsin sequences identified from PIA were assessed in Geneious, version 10 (Kearse *et al.*, 2012), for length, fragment overlap, and sequence similarity. The curated opsin sequences were added to the opsin amino acid alignment from Bok *et al.* (2017) using MAFFT (Katoh and Standley, 2014), and a new phylogeny was reconstructed using RAxML, version 8 (Stamatakis, 2006), as implemented on the CIPRES portal (Miller *et al.*, 2010). PIA-identified *S. corniculatus* sequences are available on GenBank (Table A1).

Results

Radiolar eye types and arrangements

Here we report on the known diversity of radiolar eyes of serpulids as described in previous studies as well as from

newly reported field observations. We have attempted to categorize serpulid radiolar eyes along similar lines to sabellids after Bok *et al.* (2016). In that review, we created the following categories of radiolar eyes: type S (simple ocelli), type CP (compound-paired), type CS (compound-single), and type CI (compound-inside) (Fig. 1E). Serpulids have no known analogs to type CI eyes, which in sabellids are located on the inside of the distal tips of the radioles in the genera *Acromegalomma* and *Stylomma*. However, we have created two new categories for radiolar eyes located on the operculum of serpulids: type oS (opercular-simple) and type oC (opercular-compound) (Fig. 1F). Table 1 details the types of radiolar eye arrangements found in each genus of the Serpulidae. Refer to Table S1, available online, for radiolar eye details at the species level. Usually, each species of serpulid has only a single radiolar eye arrangement type. However, in some species there is a gradient of type CP eyes diminishing distally along the radiole into type S eyes.

It should be noted that in Bok *et al.* (2016), we concluded that despite being derived from similar ciliary photoreceptor cells, sabellid radiolar eyes likely arose independently more than once in the family and possibly resulted from unique elaborations in essentially every genus that expresses radiolar eyes. Therefore, the radiolar eye arrangements in serpulids likely share no direct homology to those in sabellids, and the shared categorizations presented here are used out of convenience rather than to imply any evolutionary connection beyond convergence driven by similar anatomical features, developmental loci, or visually guided tasks. The similarities and differences between radiolar eyes in sabellids and serpulids will be addressed further in the "Discussion." Finally, many serpulids do not appear to possess superficially obvious radiolar eyes, but without exhaustive TEM surveys it is difficult to rule out the presence of unpigmented eyes in fresh tissue or in preserved tissue that has lost pigmentation. Indeed, it could be that unpigmented radiolar photoreceptors are widespread in fan worms.

Type S radiolar eyes are composed of single simple ocelli scattered irregularly or in pairs along both aboral corners of the radioles. Type S eyes are perhaps the most pervasive and are found in the genera *Crucigera*, *Metavermilia*, *Microprotula*, *Pomatostegus*, *Protula*, *Spirobranchus*, and *Vermiliopsis*. These ocelli can be very diffusely scattered on the radioles (Fig. 2A, S) or packed into dense but irregular rows along the radiolar corners (Fig. 2B, C).

Type CP radiolar eyes are paired compound eyes composed of numerous ocelli. These eyes are found distributed along the radioles as seen in some species of *Protula* (Fig. 2E) or at the base of each radiole as in some *Serpula* (Fig. 2D). These ocellar aggregations typically have fewer than a dozen facets. In *Serpula jukesi* (Baird, 1865) several ocelli are uniquely consolidated behind a single lens, creating a rudimentary simple eye (Fig. 3A).

Type CS radiolar eyes are single compound eyes on one aboral corner at the base of the two dorsalmost radioles. They are found exclusively in all species of Christmas tree worms (the *Spirobranchus corniculatus* and *Spirobranchus giganteus* species complexes) (Fig. 2F–N) and are composed of up to 1000 facets, by far the most numerous among serpulid radiolar eyes (Fig. 2J). In adults, these sophisticated eyes are partially shielded from many viewing angles by the twin spires of the well-developed radiolar crown that gives this group their name (Fig. 2G, H). However, when the crown is fully extended in feeding position, the eyes maintain a broad view primarily outward and upward along the dorsalmost surface of the worm's substrate. Also, when emerging from their tube, before fully extending the radiolar crown, *Spirobranchus* does expose its eyes to some degree (Fig. 2I). Additionally, in *Spirobranchus* juveniles or early adults, when the radioles are less pigmented and the spires are less developed, the eyes are much more exposed during normal crown extension (Fig. 2O).

Type oS eyes are single simple ocelli scattered on the brim of the operculum and are found in some *Pomatostegus* (Fig. 2P–R) and *Spirobranchus* (Fig. 2T). In *Pomatostegus stellatus* (Abildgaard, 1789), the opercular ocelli appear very similar to those found scattered on the radioles (Fig. 2R, S).

Type oC eyes are compound eyes formed from numerous ocelli located on the operculum and are found in *Pseudovermilia* and *Pyrgopolon* (multiple compound eyes with 20–30 ocelli; Fig. 2U).

The structure of serpulid radiolar ocelli

Compared to sabellids, TEM studies on the ultrastructure of serpulid radiolar ocelli are much more limited in the literature (sabellid studies reviewed in Bok *et al.*, 2016). However, the dissertation work of Smith (1985) contains previously unpublished ultrastructural descriptions of radiolar ocelli structures in five serpulid species: *Spirobranchus corniculatus* (as *Spirobranchus giganteus* (Pallas 1766); also in Smith, 1984b), *Spirobranchus tetraceros*, *Protula* sp. (as *Protula tubularia* (Montagu, 1803); for a discussion see Ben-Eliahu and ten Hove, 2011), *Serpula jukesi*, and *Protula anomala* (Day, 1955). Here we will describe these ocellar structures in detail for the first time and additionally present new TEM observations from *Pomatostegus stellatus*. Diagrammatic representations of radiolar ocelli from each of these species can be found in Figure 3A. Common features include a ciliary sensory cell invested by supporting cells that offer structural integrity to the ocellus and/or contain screening pigment granules. The supporting cells typically have apical microvilli that contribute to the cuticle and excrete lenses for the ocellus while leaving a small pore in the optical path of the sensory cell. Each sensory cell has a distal sensory segment and proximal soma that contains the nucleus, the majority of mitochondria, and other organelles. Neuronal processes extend from the base of the sensory cell soma to the radiolar nerve and presumably on to the brain. For our

Table 1

Radiolar eyes in serpulid genera

Genus	Eye type	Comments	References
Apomatus	CP	Paired compound eyes along radiole aboral corners in some species	Fauvel, 1927; ten Hove and Pantus, 1985
Crucigera	S, CS	Randomly distributed ocelli on aboral corners of radioles in some species; occasionally a single compound eye near the base of each radiole	This study
Dasynema	CP	Multiple paired compound eyes with up to 11 ocelli each along radiole aboral corners	Grube, 1878 (in Andrews, 1891); Imajima and ten Hove, 1984
Janita	?	Stalked eyes at the base of pinnules	Fauvel, 1927 (as *Omphalopoma*); Rioja, 1931 (as *Omphalopomopsis*)
Metavermilia	S	Paired single ocelli along radioles in some species	This study
Microprotula	S	Paired, probably single, ocelli along radioles in some species	Uchida, 1978
Paraprotis	CP	Paired compound eyes with only two or three ocelli each along the radiole aboral corners	Uchida, 1978
Pomatostegus	S, oS	Randomly distributed ocelli on both corners of the radioles and on the rim of the operculum	Smith, 1985; this study
Protula	CP, S	Paired compound eyes or scattered single ocelli along the outside of radiole aboral corners in many species	Claparede, 1868 (in Andrews, 1891); Radl, 1912; Pixell, 1913; Fauvel, 1927, 1953; Monro, 1933; Imajima and Hartman, 1964; Pillai, 1971; Uchida, 1978 (as *Paraprotula*); Vine and Bailey-Brock, 1984; Smith, 1985; this study
Pseudovermilia	oC	None in some species; in others numerous lenses in the wedge-shaped zone at the ventral edge of the opercular bulb	This study
Pyrgopolon	oC	Compound eyes on the opercular brim in *Pyrgopolon ctenactis* (Mörch, 1863)	ten Hove and Kupriyanova, 2009
Semivermilia	oS	A single red ocellus at the base of the opercular ampulla in *Semivermilia pomatostegoides* (Zibrowius, 1969)	Vine and Bailey-Brock, 1984
Serpula	CP	Paired clusters on the base of radioles in some species; *Serpula jukesi* consolidates multiple ocelli behind a shared lens	Smith, 1985 (*S. jukesi*); this study
Spiraserpula	S	Contradictory observations in fresh material, from up to six single eyespots in the base of lateral radioles (not the most dorsal or ventral) or red spots without lenses	This study
Spirobranchus	CS	*Spirobranchus corniculatus* and *Spirobranchus giganteus* complexes (Christmas tree worms) with large single compound eyes at the internal base of each dorsal radiole	Smith, 1985; this study
	S	*Spirobranchus tetraceros* complex with paired or irregular single ocelli along radiole aboral corners	Smith, 1985; this study
	CP	*Spirobranchus kraussii* (Baird, 1865) with paired compound ocelli spaced along radiole aboral corners	Pillai, 1971; Mak, 1982; Smith, 1985 (as *Pomatoleios kraussii*)
	oS	*Spirobranchus corrugatus* (Straughan, 1967) with scattered red ocelli on the opercular rim	Vine and Bailey-Brock, 1984; Smith, 1985 (both as *Spirobranchus* sp.); Kupriyanova *et al.*, 2015; this study
Turbocavus	CP, S	Radioles with evenly spaced single ocelli and/or ocellar clusters in *Turbocavus secretus* Prentiss, Vasileiadou, Faulwetter, Arvanitidis & ten Hove, 2014	Prentiss *et al.*, 2014
Vermiliopsis	S	Randomly distributed ocelli on both aboral corners of radioles	Pixell, 1913; Iroso, 1921 (partially under other synonymic names); Fauvel, 1927; Pillai, 1971; Smith, 1985; this study

Eye types: S, single simple ocelli; CP, compound-paired; CS, compound-single; oS, opercular simple; oC, opercular compound. Radiolar eyes not reported in *Bathyditrupa*, *Bathyvermilia*, *Chitinopoma*, *Chitinopomoides*, *Ditrupa*, *Ficopomatus*, *Filograna*, *Filogranula*, *Filogranella*, *Floriprotis*, *Galeolaria*, *Hyalopomatus*, *Hydroides*, *Josephella*, *Laminatubus*, *Marifugia*, *Neomicrorbis*, *Omphalopomopsis*, *Paumotella*, *Placostegus, Protis*, *Pseudochitinopoma*, *Rhodopsis*, *Salmacina*, Spirorbinae, *Spirodiscus*, *Tanturia*, and *Vitreotubus*.

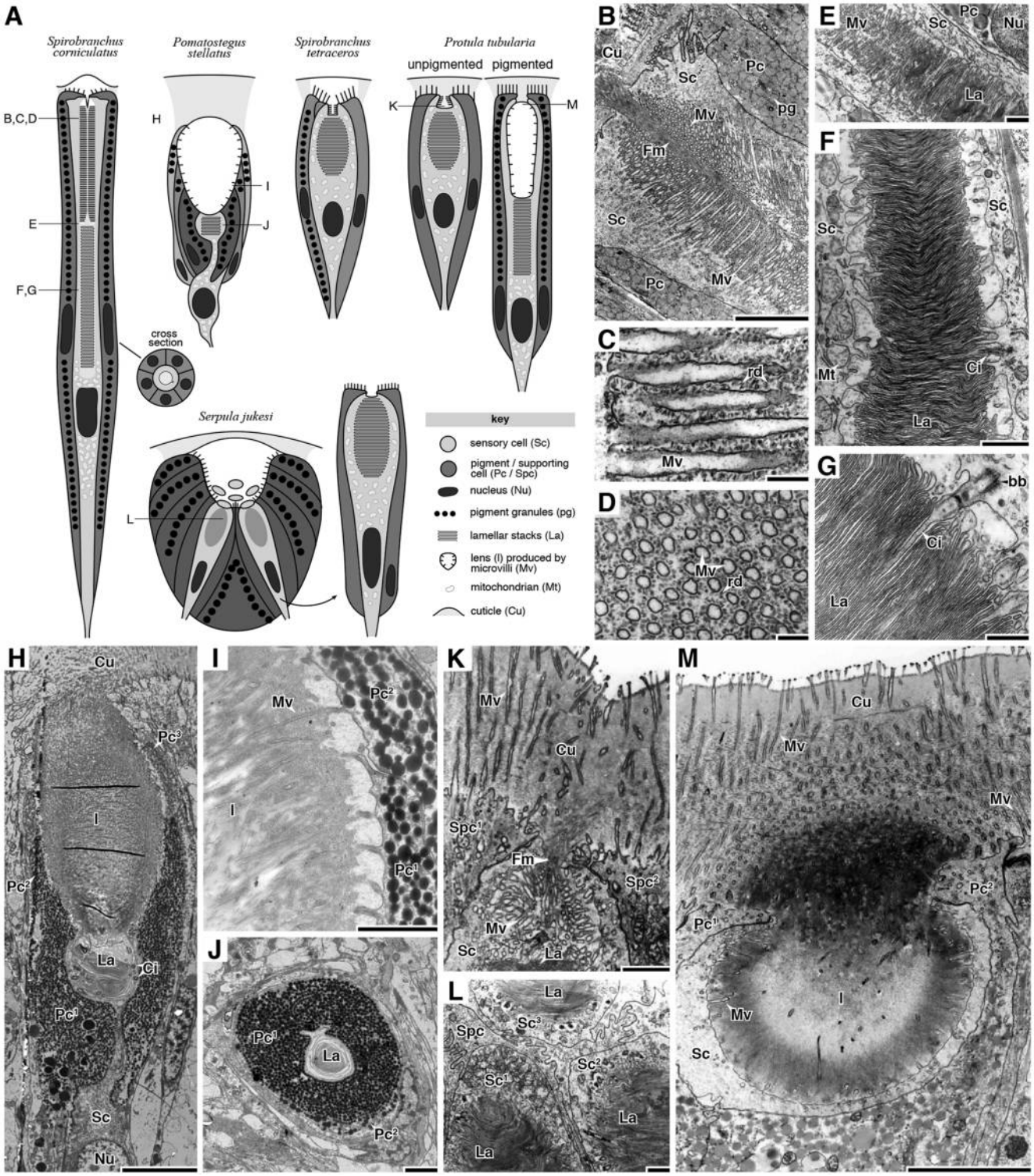

Figure 3. Serpulid radiolar ocellar structures. (A) Diagrams of radiolar ocelli from five serpulid species. Common components and cellular structures are indicated in the key. Letter labels refer to details shown in transmission electron microscopy image panels (B–M). bb, basal body; Ci, cilium; Cu, cuticle; Fm, filament; l, extracellular lens; La, lamellar stacks; Mt; mitochondrion; Mv, microvilli; Nu, nucleus; Pc, pigment cell; pg, pigment granules; rd, rodlet; Sc, sensory cell; Spc, supporting cell. (B–D) The distal region of the *Spirobranchus corniculatus* sensory cell highlighting the microvillar region of the sensory pocket. Microvilli and associated extracellular rodlets

description of ocellar fine structures, we will focus on the major details related to the optical elements, pigment cups, and sensory cells. Readers are encouraged to refer to Smith (1985) for greater detail regarding cellular ultrastructure.

Spirobranchus corniculatus has by far the most sophisticated and best examined radiolar eyes among the serpulids. Their type CS eyes contain as many as 1000 facets. Each of these facets overlays a discrete ocellus unit averaging 100 μm in length and constituted by a central sensory cell surrounded by usually five pigment cells (Fig. 3A). The pigment cells encapsulate the distal tip of the sensory cell, leaving only a small aperture connecting the sensory cell to the cuticle. The pigment cells project microvilli apically, excreting a cuticular lens. The distal half of the sensory cell produces a sensory cavity formed by a long tubelike invagination of its apical membrane. The distal half of the sensory cavity is filled with a matrix of microvilli from the sensory cell, resembling a rhabdom (Fig. 3B). The microvilli are well organized and are surrounded in the extracellular space by numerous perpendicularly aligned and presumably secreted membranous rodlets (Fig. 3C, D). The center of the rhabdom also produces a vertically extending filamentous column that passes through the aperture to the cuticular lens (Fig. 3B). About halfway down the sensory cavity the microvilli give way to densely folded, flattened lamellar stacks emerging from sensory cilia around the walls of the sensory cavity (Fig. 3E–G). The lamellar stacks continue nearly to the end of the sensory cavity, which terminates at the soma.

Pomatostegus stellatus has scattered simple ocelli appearing on the radioles (type S) as well as on the opercular brim (type oS). These ocelli appear similar in the two areas but vary among themselves slightly in size and pigmentation (Fig. 2R). The general ultrastructure of the ocelli on the radioles and operculum is indistinguishable. Each ocellus is formed by a single sensory cell and up to two or four surrounding pigmented supporting cells (Fig. 3A, H). The pigment cells contribute microvilli into the optical path, secreting a granular, conical lens that lies well below the cuticle surface, which is produced by surrounding epithelia cells. There is no cuticular lens, and the cuticle surface overlying the ocelli is flush. The pigment cells are arranged in a nested, tiered configuration, with the innermost pigment cell encapsulating the sensory cavity and contributing to the proximal segment of the lens (Fig. 3H). Additional pigment cells contribute to more distal stretches of the lens, and their pigment granules become decreasingly electron dense (Fig. 3I). Thus, the number of pigment cells encapsulating each ocellus may explain the differences in size and coloration. The sensory cell is unusual compared to other serpulids. The soma is located outside of the pigment sheath, through which it projects a narrow cytoplasmic channel that expands into a sensory chamber filled with whorled lamellae produced by sensory cilia (Fig. 3H, J).

Spirobranchus tetraceros radiolar ocelli are an example of perhaps the most rudimentary design. They occur in diffuse rows of around 10 ocelli in a type S configuration, with the greatest number of ocelli located on the dorsalmost radioles. An ocellus consists of a single sensory cell surrounded by a number of supporting cells with variable pigmentation (Fig. 3A). The apical microvilli from the supporting cells produce the cuticle as well as a cuticular lens that is flush externally and convex on its inner surface. An unpigmented supporting cell encircles the apex of the sensory cell. The sensory cell has a distal sensory segment and a proximal soma. The sensory segment is formed by an apical invagination around 12 μm in depth and filled with whorled lamellae produced by sensory cilia on the sides of the cavity. In the distalmost segment of this sensory cavity the lamellae give way to a small array of microvilli. It should be noted that *S. tetraceros* is presently regarded to be a complex of species, and Smith (1985) reported possible specific variation in ocelli distribution, including absence of ocelli in some individuals.

Members of *Protula* have rows of type S diffuse single radiolar ocelli on both sides of the radioles. In addition to pigmented ocelli, *Protula* also has unpigmented photoreceptors that are not superficially visible and were discovered by chance during TEM investigations of the pigmented ocelli (Fig. 3A). The pigmented ocelli are composed of a sensory cell whose distal sensory cavity is surrounded by a pair of pigmented supporting cells. Uniquely in this species, the apical microvilli of the supporting cells do not produce a cuticular lens. Rather, the distal half of the sensory cell cavity contains microvilli that secrete a lens into the cavity (Fig. 3M). Below the lens, whorled and folded lamellae contributed by sensory cilia fill the sensory cavity. The *Protula* unpigmented photoreceptors are generally comparable to *Spirobranchus tetraceros* but lack pigmented supporting cells and a cuticular lens. Like *S. tetraceros*, the unpigmented ocellus sensory cavity is filled with whorled lamellae and a small microvillar matrix at the distal pore encircling a filamentous mass (Fig. 3K). Similar pigmented radiolar ocelli were also found in *P. anomala* (see Smith, 1985).

are shown in (C) longitudinal and (D) transverse section. (E) The transition zone in the *S. corniculatus* sensory cell between the distal microvillar and proximal lamellar regions. (F, G) The proximal lamellar region of the sensory cell of *S. corniculatus*. (H) The opercular ocellus from *Pomatostegus stellatus*. (I) The pigment cells that secrete the extracellular lens are shown, as well as (J) a cross section through the sensory pocket. (K) The distal region of the *Protula* unpigmented ocellus including the microvillar pocket and cuticle. (L) A cross section through the radiolar eyelet of *Serpula jukesi* with three sensory cells visible. (M) The cuticle and lens of the *Protula* pigmented ocellus. Scale bars: (B, J, M) = 2 μm; (C, D) = 250 nm; (E, F, I, K, L) = 1 μm; (G) = 500 nm; (H) = 5 μm.

Serpula jukesi has radiolar eyes unlike any other described serpulid. Instead of having scattered single ocelli or grouping ocelli together into a compound eye, *S. jukesi* has radiolar eyes with four to six sensory cells and their supporting cells placed behind a single shared lens in a continuous pigment cup (Fig. 3A, L). These simple eyes occur in a pair near the base of each radiole. The lens is produced by microvillar projections from the supporting cells alone and is flush with the cuticular surface and convex internally along the margin of the pigment cup. The cluster of sensory cells lies below the lens at the bottom of the pigment cup. Each sensory cell is ensheathed by three mostly unpigmented supporting cells that also contribute to producing the lens. The sensory cells themselves are divided into a proximal soma and a larger distal sensory segment. The sensory cavity is 16 μm in depth and filled with stacked and whorled lamellae contributed from sensory cilia on all sides of the cavity.

Spirobranchus corniculatus *visual pigment absorbance spectra*

We used MSP to measure the spectral absorbance of photoreceptors in the *S. corniculatus* type CS compound eye. We obtained clean post-bleach photoconversions for seven photoreceptors. The raw pre- and post-bleach difference spectra were averaged and fitted with a visual pigment template curve based on the equations of Stavenga *et al.* (1993). This had a wavelength of maximum absorbance (λ_{max}) of 464 nm (Fig. 4A). The λ_{max} range of template fits for individual scans was between 450.2 and 472.3 nm, so there is the possibility for the existence of multiple visual pigments (Fig. A2). However, it should be noted that the best fits with the strongest photoconversions all had λ_{max} above 460 nm, making 450.2 nm a slight outlier.

This visual pigment, with λ_{max} = 464 nm, is well suited for operating in the shallow marine habitats of *S. corniculatus* (Fig. 4B, thin gray lines representing idealized downwelling irradiance spectra at increasing depths). We also obtained MSP transmission spectra for the orange pigment in the *S. corniculatus* pigment cells (Fig. 4B, thin black line), which blocks most light below 550 nm and efficiently acts as a screening pigment for the blue-green-absorbing visual pigment in the marine habitat. We also observed that we were able to record photoconversions only from the proximal, presumably lamellar, region of the photoreceptor. We did not obtain photoconversions in the more distal segment of the photoreceptor sensory cavity that contains microvilli (see Fig. 2A–D) despite bleaching periods of up to 7 min.

Transcriptomic sequencing of Spirobranchus corniculatus *radiolar eye*

We used transcriptomic sequencing to identify proteins putatively involved in the phototransduction cascade in the radiolar eyes of *S. corniculatus*. Metazoan visual systems detect light using membrane-embedded visual pigments formed by the coupling of opsin G-protein-coupled receptors and light-sensitive chromophores. Transduction occurs when a photon is absorbed by the chromophore, causing a conformational change in the visual pigment, activating a G protein and thus propagating a cellular signal along a cascade of downstream enzymes, channel proteins, and signaling molecules.

We recovered three opsin contigs from the transcriptome of six *S. corniculatus* radiolar eyes. One of the sequences, *S. corniculatus* opsin 1, was a full-length transcript (375 amino acids). The remaining 2 contigs were fragments of the last 140 and 122 amino acids of the C-tail, respectively. Additionally, the smallest recovered contig was identical in amino acid sequence to the longer C-tail fragment. Therefore, we treated these two fragments as a single opsin transcript, *S. corniculatus*

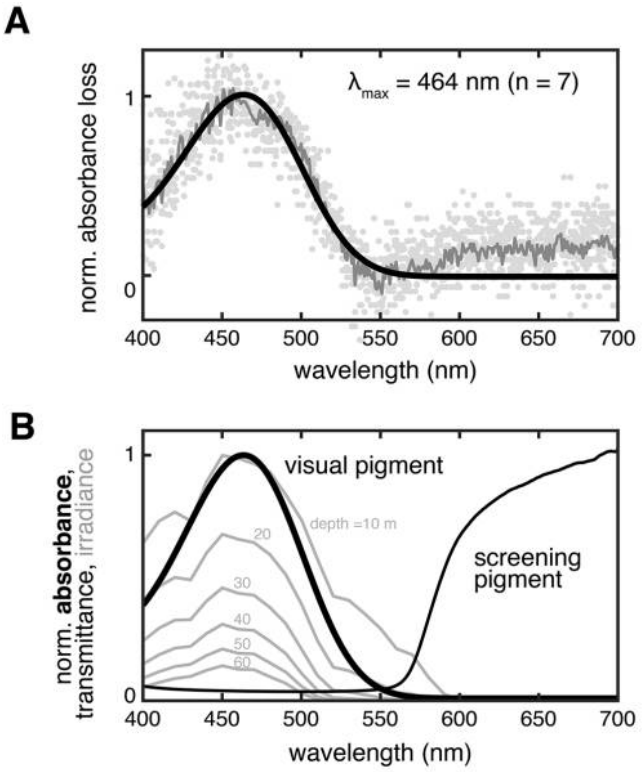

Figure 4. *Spirobranchus corniculatus* visual pigments. (A) Normalized and baselined pre- and post-bleach microspectrophotometry (MSP) difference spectra of *S. corniculatus* radiolar eye ocellar visual pigments. Plotted are seven individual difference spectra (dots), their average difference spectrum (gray line), and their best-fit visual pigment template (black line) (Stavenga *et al.*, 1993). The visual pigment's wavelength of maximum absorbance (λ_{max}) is 464 nm (n = 7). (B) A normalized spectral plot of the λ_{max} = 464 nm visual pigment from (A) (thick black line), the transmission spectrum of the screening pigment (thin black line), and the ideal absolute downwelling irradiance spectra of seawater at increasing depths (10–60 m; thin gray lines). The downwelling irradiance spectra were calculated using clear water attenuation coefficients from Smith and Baker (1981) with a D65 International Commission on Illumination (CIE) solar illuminant standard.

opsin 2 (Fig. 5; Table A1). Phylogenetically, opsin proteins generally fall into four major clades: G_q-opsins, tetraopsins, c-opsins, and xenopsins (Porter *et al.*, 2012; Ramirez *et al.*, 2016). The two *S. corniculatus* opsin sequences are very similar (96.4% amino acid identity), falling out with a cluster of poorly understood opsins at the base of the c-opsin clade, which we have termed invertebrate c (InvC)-opsins. In this opsin phylogeny InvC sequences form a monophyletic clade, but it is poorly supported; and in some cases this group is recovered as a number of basally branching paraphyletic clades separated by taxa: panarthropods, echinoderms, and annelids (Bok *et al.*, 2017). Previous transcriptomic sequencing efforts have shown that the sabellid *Acromegalomma interruptum* (Capa & Murray, 2009) expresses a similar InvC-opsin in its radiolar eyes (Bok *et al.*, 2017; as *Megalomma interrupta*).

Figure 5B also indicates the amino acid residue present at bovine rhodopsin position 94 for each InvC-opsin. This residue has been implicated in ultraviolet spectral tuning in *Platynereis dumerilii* InvC-opsin 2 (Tsukamoto *et al.*, 2017). A lysine (K) at this position shifts the visual pigment's maximum absorbance into the ultraviolet range. *Spirobranchus corniculatus* InvC-opsin 1 has a serine (S) residue at this position. We did not recover this sequence region from *S. corniculatus* InvC-opsin 2.

We also recovered a number of transcripts related to phototransduction cascade components. Notably, we recovered three G-protein alpha subunits: $G\alpha_o$, $G\alpha_i$, and $G\alpha_s$ (Table A1). Additionally, we recovered transcripts homologous to the G-protein beta subunit, the G-protein gamma subunit (*gngt1*), protein kinase C (*PKC*), cyclic nucleotide gated-channel alpha 1 (*cnga1*), regulator of G-protein-signaling 9 (*RGS9*), retinal degeneration B (*rdgB*), arrestin (*arr*), guanylyl cyclase (*GC*), and cyclic nucleotide phosphodiesterase (*PDE6abc*)—all of which are implicated with phototransduction in ciliary-type photoreceptor cell systems (Fain *et al.*, 2010). Furthermore, our sequencing identified a number of transcription factors implicated in eye development (*Pax6*, *eya*, *six4*, *so*, *glass*, *dpp*), as well as two cryptochrome (*cry*) transcripts, which code for light-sensitive proteins usually involved in the entrainment of circadian rhythms.

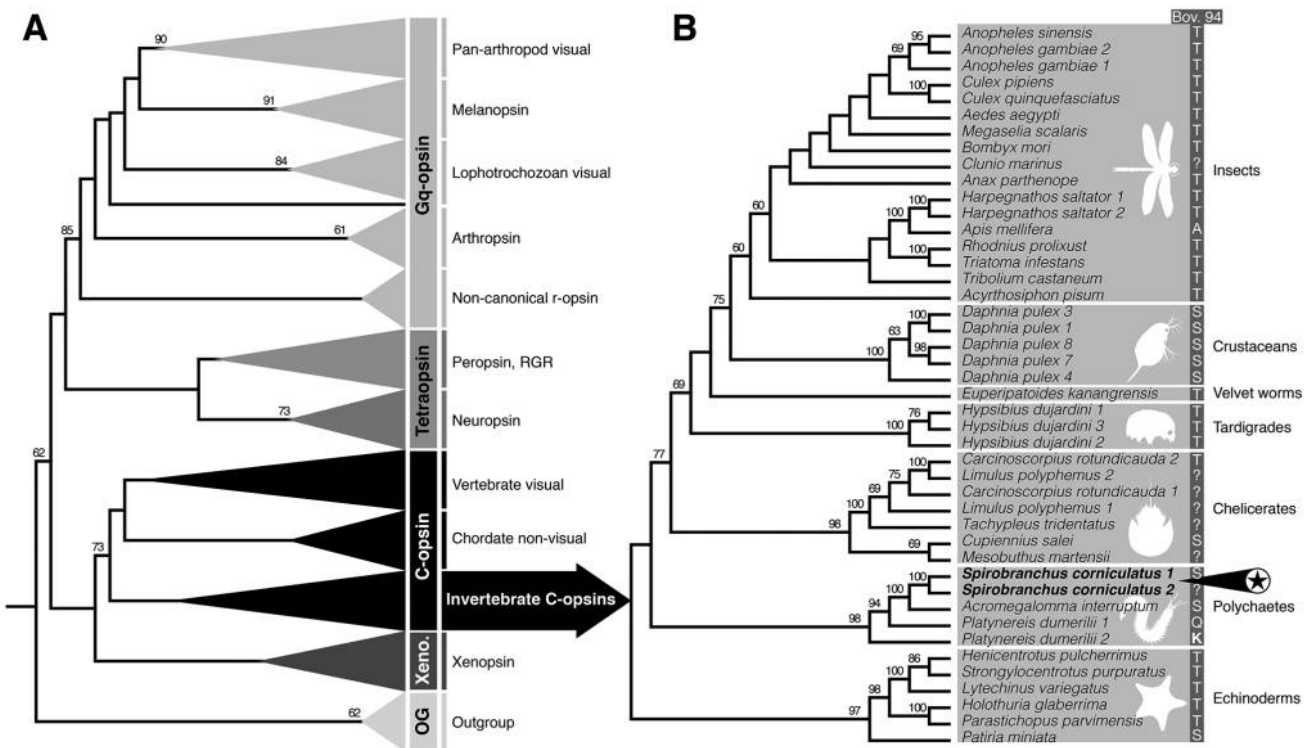

Figure 5. *Spirobranchus corniculatus* radiolar eye opsins. (A) Maximum likelihood cladogram of metazoan opsins with collapsed subclades and shading to indicate the four main opsin clades; G_q-opsins, tetraopsins, c-opsins, and xenopsins. Phylogeny based on sequences from Bok *et al.* (2017), opsin clades after Ramirez *et al.* (2016). (B) The expanded invertebrate c-opsin (InvC) clade showing all included sequences as well as their taxonomic affiliation. The two *S. corniculatus* radiolar eye opsin sequences are in bold and marked with a star. The residue present at the site corresponding to bovine rhodopsin position 94 for each sequence is also indicated. A lysine (K) at this site is implicated in ultraviolet tuning of the brain-expressed *Platynereis dumerilii* InvC-opsin 2 (Tsukamoto *et al.*, 2017).

Discussion

Structural comparison of serpulid ocelli

Serpulid photoreceptor sensory cells appear similar across the family, suggesting a conserved origin. The photoreceptor cells always display a distal sensory segment containing the lamellae-packed sensory cavity and proximal soma. The soma is typically continuous with the sensory segment, except in *Pomatostegus stellatus*, where a narrow channel between enveloping pigment cells connects the sensory segment and soma (Fig. 3H). The cilia-derived lamellae in the sensory cavity are identical in structure and appearance across the family, but their packing varies between stacked, folded, and whorled configurations. Furthermore, there are a great deal of additional ultrastructural similarities among serpulid photoreceptors, discussed in detail in Smith (1985). It is likely that all serpulid branchial photoreceptors share a common origin from an epidermal ciliated sensory cell, not unlike the chemo- or mechanosensory cells found throughout the length of the radioles, also in the aboral corners (Smith, 1985). At some point one such cilium may have gained opsin photopigment expression and light sensitivity, followed by invagination of the apical surface into a sensory cavity where increasingly folded whorls of ciliary lamellae could be stacked, producing a rudimentary ocellus akin to the *Protula* unpigmented ocellus.

Beyond the sensory cell, however, the serpulid ocelli vary greatly, suggesting that despite apparently starting with similar radiolar photoreceptor cells, ocelli arose and elaborated more than once in the family. In general, serpulid receptors are roughly analogous to ommatidia in arthropod apposition compound eyes, with a single lens element passing light into a single sensory cavity, fully shielded by screening pigment in the supporting cells. Beyond that, the structure of radiolar ocelli vary greatly among serpulid species. The number of supporting pigment cells forming the screening pigment cup can be as many as six in *Spirobranchus corniculatus* to none in the *Protula* unpigmented receptor. Likewise, the nature and origin of the lens are inconsistent among species surveyed—though it is thought to typically be composed of glycogen or cuticular materials. In *S. corniculatus*, *Pomatostegus stellatus*, *Spirobranchus tetraceros*, and *Serpula jukesi* the lens is likely produced by excretion from microvilli on the supporting pigment cells. Among these, *S. corniculatus*, *S. tetraceros*, and *S. jukesi* produce a cuticular lens above the ocellus while *P. stellatus* creates a recessed conical lens, below the flat cuticular surface and enveloped by the pigment cup of the ocellus. The *Protula* pigmented ocellus also has a recessed conical lens of this nature; however, it is apparently excreted by microvilli emerging from the distal segment of the sensory cell, instead of the supporting cells.

There has been some discussion regarding the rhabdom-like microvillar region in the distal half of the *Spirobranchus corniculatus* sensory cavity (Fig. 3B–D). Smith (1984b, 1985) suggested that these microvilli could serve some photoreceptive function in tandem with the more distal ciliary lamellar stacks. A popular notion in current vision research is that some photoreceptors may contain multiple simultaneous phototransduction cascades, perhaps locally regulating sensitivity adaptation or performing simple chromatic comparisons (Su *et al.*, 2006; Vöcking, 2016). The rhabdomeric and ciliary membrane elaborations of the *S. corniculatus* sensory cavity make such a system a very attractive possibility in this case. However, we find it highly unlikely that this microvillar region serves a photoreceptive purpose for several reasons. (1) We were unable to obtain MSP photoconversions when scanning more distal regions of the sensory cavities. (2) Transcriptomic sequencing from these eyes yielded only InvC-opsins and ciliary phototransduction cascade components (Fig. 5). Rhabdomeric photoreceptors are known to achieve photoreception only *via* G_q-opsins and a specialized microvillar phototransduction cascade (Fain *et al.*, 2010), no components of which were identified by our sequencing efforts. (3) The rhabdom is not as densely packed with microvilli as we would expect from an optimized photoreceptor, as in the cerebral ocelli, for instance (Fig. A1). Much space is instead reserved for the unusual rodlets that encircle the microvilli (Fig. 3C, D).

We instead propose that the rhabdomeric region of the *S. corniculatus* ocellus may act in some optical role. The regularity of the microvilli and their rodlets, as well as the filament column, may serve as some sort of light guide. Alternatively, the microvillar region may function as a spacer along with the pigment cup to restrict the light acceptance angle of the lamellar stacks farther down in the sensory cavity. Such a spacer would then open adaptive space where a lens could be added, as we see with the *Protula* pigmented ocellus (Fig. 3M). Some microvillar elaboration is found on the distalmost segment of the sensory cavity in most serpulid photoreceptors cells, besides *Pomatostegus stellatus*, where this was not observed. In *Spirobranchus tetraceros* and the unpigmented *Protula* ocelli, this microvillar region is diminutive but regardless appears to partially contribute to an excreted filament and perhaps some granular glycogenic material, continuous with the overlaying cuticular lens produced by the supporting cells. (Fig. 3K). The *S. corniculatus* rhabdom appears to be homologous to, yet highly elaborated from, these small microvillar arrays.

Function of serpulid radiolar eyes

What can serpulids see? For the majority of species surveyed, the radiolar eyes likely suffer from poor spatial resolution. Instead, they seem to have prioritized redundancy, broad coverage, and rapid, specialized processing in service to their single, robust withdrawal behavior.

Correlating form to function, we can assume the majority of serpulids are capable of little more than rudimentary shadow detection. The scattered single type S/oS ocelli and compound

eyes found in most genera likely trigger a withdrawal response once a certain threshold of ocelli responding to a decrease in illumination is crossed. Though rigorous light response experiments have not been carried out in serpulids, Nicol (1950) reported that the sabellid *Acromegalomma vesiculosum* (Montagu, 1813) (as *Branchiomma*) responded most dramatically when a shadow stimulus was moving. Similar field and aquarium observations were reported by Smith (1985) for *Spirobranchus corniculatus*. Movement discrimination in fan worm radiolar eyes could be facilitated with little processing expense by an object gradually infringing on the field of view of increasing numbers of ocelli, until some threshold is crossed. However, in essentially every example, the poor organization and semirandom distribution of ocelli preclude the serpulids from visually guided tasks beyond shadow or motion detection. Even the paired radiolar or opercular compound eyes (type CP/oC) lack the organization or facet counts required for resolving vision. Instead, these simple compound eyes probably function similarly to the type S eyes, except with a slight advantage in shared screening pigment and a distribution of fields of view that are less likely to redundantly overlap.

Nilsson (1994) suggested that the radiolar eyes in sabellids and serpulids function as a sort of "burglar alarm," responding to decreasing illumination or a moving silhouette in the water column and triggering the rapid withdrawal response. This notion is supported by behavioral observations of sabellids by Nicol (1950), who found *A. vesiculosum* (as *Branchiomma*) responding with a withdrawal response to decreases in illumination only. Furthermore, Leutscher-Hazelhoff (1984) recorded hyperpolarizing photic responses from the radiolar photoreceptors of *A. vesiculosum* (as *Branchiomma*). It has been argued that a hyperpolarizing response is a rule for ciliary photoreceptors and the natural choice for a shadow detector, since a decrease in illumination would produce a proper depolarizing neural signal (Hartline, 1938; Fain *et al.*, 2010). It could be that early metazoans possessed both a ciliary photoreceptor for bright-light vision and shadow detection, as well as an adaptable microvillar photoreceptor geared toward dim-light vision. Our observations of a $\lambda_{max} = 464$ nm visual pigment in *Spirobranchus corniculatus* indicate that these photoreceptors appear to be closely tuned to the dominant wavelengths of light in shallow marine habitats (Fig. 4B). This further supports the notion that these fan worm photoreceptors function as a shadow or silhouette detector against the prevailing bright-illumination conditions of the shallow seas. The identification of at least two expressed InvC-opsin transcripts in *S. corniculatus*, along with the observed variation in measured λ_{max}, offers the intriguing possibility of multiple spectrally distinct photoreceptor types contributing to shadow detection in the variable underwater light environment.

A notable exception to the distributed and poorly organized radiolar eyes in the majority of serpulids are the type CS eyes of *S. corniculatus* and other Christmas tree worms, which possess at a minimum the structural sophistication required for rudimentary resolving vision. These consolidated compound eyes can contain up to 1000 well-organized facets that produce a distinct pseudopupil (Fig. 2L), suggesting the possibility for some spatial analysis. Despite their apparent sophistication, it would be easy to conclude from both the shape and position of the compound eyes that they are not well suited for advanced visual function. Unique among compound eyes, each eye is concave along the major axis, twisted inward, and buried underneath much of the branchial crown when it is deployed in feeding position. Of course, the concave eye structure might only be an economical drawback, as the atypical bean shape does not necessarily hinder the potential for spatial resolution performance. Additionally, their placement at the base of the crown keeps these major sensory organs in the safest possible location in the event of a successful predatory attack.

Field and unpublished observations (Smith, 1985) suggest that the Christmas tree worm compound eye is indeed capable of mediating more complex visual behavior than basic shadow response and the detection of conspicuous overhead motion. Worms have been observed to withdraw on the approach of fish species known to predate on them with no shadows having been cast and without displaying the same response to other fish species swimming in the same area. Further research is required to determine whether the structural sophistication of the Christmas tree worm compound eye indeed translates to advanced visual functions or is merely an odd evolutionary approach to the standard serpulid "burglar alarm."

As with serpulids, in the majority of sabellid genera the radiolar ocelli or eyes are arrayed in a manner that seems counterintuitive, scattered in the dozens or hundreds along the outside corners of every radiole. Only some species of the sabellid *Acromegalomma* possess an economical pair of large eyes prominently positioned on the tips of the dorsalmost radioles—offering the potential for high visual performance with full viewing angles and little redundancy. However, these eyes are more vulnerable, and the cost of their loss is high, so the distributed, redundant eye approach may be preferable for the role of shadow detection.

Serpulids also have the opportunity for an additional visual strategy in their operculum. The operculum could logically serve as a sort of periscope, emerging first from the tube and being prominently positioned once extended. Indeed, several serpulids make use of this strategy (Fig. 2Q–U; Table 1); and considering the operculum's shared ontological history with the radioles, it is unsurprising that the ocelli found on these two parts of the crown were observed to be homologous in *Pomatostegus stellatus*.

Evolutionary context of serpulid radiolar eyes

Our comparison of radiolar eye types throughout the serpulids suggests that they serve as a weaker phylogenetic character than in sabellids (Bok *et al.*, 2016), where eye ar-

rangement and ocellar structure are well conserved within genera. It should be noted that there is currently poor resolution in the phylogeny, and the taxonomy of serpulid species is confused. However, comparisons of radiolar eye arrangement with most current serpulid taxonomies clearly suggest that radiolar eyes or ocelli have been gained, lost, and elaborated multiple times within the family. Beyond this, it is difficult to make a clear assessment of radiolar eye evolution in the serpulids at this time. Interestingly, a similar plasticity is hypothesized for the ontogeny of the operculum, being derived from a radiole in the *Serpula*/*Hydroides*/*Crucigera* clade in serpulins but a *de novo* development from the prostomium in spirorbins (Brinkmann and Wanninger, 2009).

Comparison of radiolar ocellar fine structure, developmental history, and expression location throughout the serpulids suggests a shared ancestry for these photoreceptors, with subsequent elaborations to the supporting cells and optical elements emerging uniquely in different species (Fig. 3). Furthermore, this ciliary photoreceptor also appears to be structurally homologous to those found in the radiolar eyes of sabellids (Bok *et al.*, 2016). This is further supported by close opsin sequence homology between the InvC-opsins found in the sabellid *Acromegalomma interruptum* and the serpulid *Spirobranchus corniculatus* (Fig. 5). InvC-opsins are primarily found in the neural and distributed visual systems of panarthropods, echinoderms, and annelids (Fig. 5B; Bok *et al.*, 2017), but little is understood about their function. The fan worm radiolar eye InvC-opsins are most closely related to a brain photoreceptor-expressed opsin in the errant polychaete *Platynereis dumerilii*, where it is likely involved only in simple illuminance assessment (Arendt *et al.*, 2004). To our knowledge, the sabellids and serpulid radiolar eyes are the first example of InvC-opsin expression in an animal's primary visual system.

Recently, it was discovered that the InvC-opsin in *P. dumerilii* produces a visual pigment maximally sensitive to 383-nm ultraviolet light based on the presence of a lysine residue at bovine rhodopsin position 94 (Tsukamoto *et al.*, 2017). In metazoan opsins, ultraviolet sensitivity is typically conferred by a lysine residue at positions 86, 89, 90, or 94 (reviewed in Cronin and Bok, 2016). Lysine is not present at position 94, or any of the other ultraviolet tuning sites in the InvC-opsins of *Spirobranchus corniculatus*, *Acromegalomma interruptum*, or any other species besides *P. dumerilii* (Fig. 5B). This is consistent with our measurements of a visual pigment maximally sensitive to blue-green light (464 nm) in *S. corniculatus* (Fig. 4).

Interestingly, *S. corniculatus* expresses at least two or three opsin transcripts in the radiolar eyes, compared with the single transcript found in *A. interruptum* (see Bok *et al.*, 2017, as *Megalomma interrupta*) (Table A1). Furthermore, while *A. interruptum* predominantly expresses $G\alpha_o$, *S. corniculatus* radiolar eyes have greater expression of $G\alpha_i$ (Table A1). Both of these G-protein alpha subunits are implicated in phototransduction in ciliary photoreceptors, but it is nonetheless interesting that the radiolar photoreceptors of sabellids and serpulids, apparently homologous in so many ways, may have seized on slightly different phototransduction machinery. Additional work is required to confirm which G-proteins are at work in the radiolar eye photoreceptors of both of these families.

Distributed visual systems are common in a number of invertebrate taxa including bivalves (Nilsson, 1994; Speiser and Johnsen, 2008a, b), chitons (Speiser *et al.*, 2011; Li *et al.*, 2015), starfish (Garm and Nilsson, 2014), and sea urchins (Yerramilli and Johnsen, 2010; Ullrich-Lüter *et al.*, 2011). As with the fan worms, these visual systems are mostly relevant to triggering defensive responses (Nilsson, 2013), but some may also play a role in navigation for the motile groups. These diverse distributed visual systems undoubtedly represent convergence upon a common method of detecting potential threats in the aquatic environment. It is possible that distributed visual systems represent an ideal method of producing redundant, flexible, and resilient light sensors that require minimal central processing in order to initiate a fast and robust defensive response.

Acknowledgments

We are grateful to Thomas W. Cronin for use of his microspectrophotometer, Eva Landgren for assistance with transmission electron microscopy preparation, and Maria Capa for assisting with some animal collection. MJB and D-EN are supported by the Knut and Alice Wallenberg Foundation and the Swedish Research Council. MJB was also supported by the John and Laurine Proud Foundation and the Australian Museum's Lizard Island Research Station. MLP is supported by National Science Foundation grants DEB1556819 and DEB1532382. We also thank the staff of the Carrie Bow Cay Field Station, Belize, and the Lizard Island Research Station, Australia, for assistance with field research and collection.

Literature Cited

Abildgaard, P. C. 1789. Beschreibung einer grossen Seeblase (*Holothuria priapus* Linn.) zween Arten des Steinbohrers (*Terebella* Linn.), einer grossen Sandröhre (*Sabella* Linn.). *Schr. Ges. Naturfr. Freunde Berl.* **9:** 133–146.

Andrews, E. A. 1891. Compound eyes of annelids. *J. Morphol.* **5:** 271–299.

Arendt, D., K. Tessmar-Raible, H. Snyman, A. W. Dorresteijn, and J. Wittbrodt. 2004. Ciliary photoreceptors with a vertebrate-type opsin in an invertebrate brain. *Science* **306:** 869–871.

Audouin, J. V., and H. Milne Edwards. 1834. *Annélides*, pt. 1. *Recherches pour servir à l'Historie naturelle du litoral de la France, ou Recueil de mémoires sur l'anatomie, la physiologie, la classification et les moeurs des animaux des nos côtes; ouvrage accompagné de planches faites d'après nature*, vol. 2. Crochart, Paris.

Baird, W. 1865. On new tubicolous annelids, in the collection of the British Museum, pt. 2. *Zool. J. Linn. Soc.* **8:** 157–160.

Ben-Eliahu, M. N., and H. A. ten Hove. 2011. Serpulidae (Annelida: Polychaeta) from the Suez Canal—from a Lessepsian migration perspective (a monograph). *Zootaxa* **2848:** 1–147.

Bok, M. J., and D.-E. Nilsson. 2016. Fan worm eyes. *Curr. Biol.* **26:** R907–R908.

Bok, M. J., M. L. Porter, A. R. Place, and T. W. Cronin. 2014. Biological sunscreens tune polychromatic ultraviolet vision in mantis shrimp. *Curr. Biol.* **24:** 1636–1642.

Bok, M. J., M. Capa, and D.-E. Nilsson. 2016. Here, there and everywhere: the radiolar eyes of fan worms (Annelida, Sabellidae). *Integr. Comp. Biol.* **56:** 784–795.

Bok, M. J., M. L. Porter, and D.-E. Nilsson. 2017. Phototransduction in fan worm radiolar eyes. *Curr. Biol.* **27:** R698–R699.

Brinkmann, N., and A. Wanninger. 2009. Neurogenesis suggests independent evolution of opercula in serpulid polychaetes. *BMC Evol. Biol.* **9:** 270.

Capa, M., and A. Murray. 2009. Review of the genus *Megalomma* (Polychaeta: Sabellidae) in Australia with description of three new species, new records and notes on certain features with phylogenetic implications. *Rec. Aust. Mus.* **61:** 201–224.

Capa, M., P. Hutchings, M. Teresa Aguado, and N. J. Bott. 2011. Phylogeny of Sabellidae (Annelida) and relationships with other taxa inferred from morphology and multiple genes. *Cladistics* **27:** 449–469.

Cavanaugh, G. M. 1956. *Formulae and Methods IV of the Marine Biological Laboratory Chemical Room*. Marine Biological Laboratory, Woods Hole, MA.

Claparède, E. 1868. *Les Annélides Chétopodes du Golfe de Naples, Première et Séconde partie*. Ramboz et Schuchardt, Genève et Bâle.

Cronin, T. W. 1985. The visual pigment of a stomatopod crustacean, *Squilla empusa*. *J. Comp. Physiol. A* **156:** 679–687.

Cronin, T. W., and M. J. Bok. 2016. Photoreception and vision in the ultraviolet. *J. Exp. Biol.* **219:** 2790–2801.

Cronin, T. W., and N. J. Marshall. 1989. Multiple spectral classes of photoreceptors in the retinas of gonodactyloid stomatopod crustaceans. *J. Comp. Physiol. A* **166:** 261–275.

Day, J. H. 1955. The Polychaeta of South Africa, pt. 3. Sedentary species from Cape shores and estuaries. *Zool. J. Linn. Soc.* **42:** 407–452.

DeVantier, L. M., R. E. Reichelt, and R. H. Bradbury. 1986. Does *Spirobranchus giganteus* protect host *Porites* from predation by *Acanthaster planci*: predator pressure as a mechanism of coevolution? *Mar. Ecol. Prog. Ser.* **32:** 307–310.

Dragesco-Kernéis, A. 1980. Taches oculaires segmentaires chez *Dasychone* (Annélides Polychètes) étude ultrastructurale. *Cah. Biol. Mar.* **21:** 287–302.

Ermak, T. H., and R. M. Eakin. 1976. Fine structure of the cerebral and pygidial ocelli in *Chone ecaudata* (Polychaeta: Sabellidae). *J. Ultrastruct. Res.* **54:** 243–260.

Fain, G. L., R. Hardie, and S. B. Laughlin. 2010. Phototransduction and the evolution of photoreceptors. *Curr. Biol.* **20:** R114–R124.

Fauvel, P. 1927. Polychètes se´dentaires. Addenda aux errantes, Archianne´lides, Myzostomaires. *Faune Fr.* **16:** 1–494.

Fauvel, P. 1953. *Fauna of India, Pakistan, Ceylon, Burma and Malaya:* Annelida polychaeta. Indian Press, Allahabad.

Fischer, A. 1963. Über den Bau und die Hell-Dunkel-Adaptation der Augen des Polychäten *Platynereis dumerilii*. *Cell. Tissue Res.* **61:** 338–353.

Garm, A., and D.-E. Nilsson. 2014. Visual navigation in starfish: first evidence for the use of vision and eyes in starfish. *Proc. R. Soc. Biol. Sci. B* **281:** 20133011.

Grube, A. E. 1862. Mittheilungen ueber die Serpulen, mit besonderer Berueckssichtigungihrer Deckel. *Schles. Ges. Breslau Jahresber.* **39:** 53–69.

Grube, A. E. 1878. Annulata Semperiana: Beiträge zur Kenntnis der Annelidenfauna der Philippinen, nach den von Herrn Prof. Semper mitgebrachten Sammlungen. *Mem. Acad. Imp. Sci. St. Petersb. Ser. 7* **25:** 1–300.

Hartline, H. K. 1938. The discharge of impulses in the optic nerve of *Pecten* in response to illumination of the eye. *J. Cell. Comp. Physiol.* **11:** 465–478.

Hesse, R. 1899. Untersuchungen über die Organe der Lichtempfindung bei niederen Tieren. V. Die Augen der polychäten Anneliden. *Z. Wiss. Zool.* **65:** 446–516.

Imajima, M., and O. Hartman. 1964. The polychaetous annelids of Japan. *Occas. Pap. Allan Hancock Found.* **26:** 1–452.

Imajima, M., and H. A. ten Hove. 1984. Serpulinae (Annelida, Polychaeta) from the Truk Islands, Ponape and Majuro Atoll, with some other new Indo-Pacific records. *Proc. Jpn. Soc. Sys. Zool.* **27:** 35–66.

Iroso, I. 1921. Revisione dei Serpulidi e Sabellidi del Golfo di Napoli. *Publ. Stn. Zool. Napoli* **3:** 47–91.

Katoh, K., and D. M. Standley. 2014. MAFFT: iterative refinement and additional methods. *Methods Mol. Biol.* **1079:** 131–246.

Kearse, M., R. Moir, A. Wilson, S. Stones-Havas, M. Cheung, S. Sturrock, S. Buxton, A. Cooper, S. Markowitz, C. Duran *et al.* 2012. Geneious Basic: an integrated and extendable desktop software platform for the organization and analysis of sequence data. *Bioinformatics* **28:** 1647–1649.

Kupriyanova, E. K., and T. A. Macdonald. 2006. Phylogenetic relationships within Serpulidae (Sabellida, Annelida) inferred from molecular and morphological data. *Zool. Scr.* **35:** 421–439.

Kupriyanova, E. K., and E. Nishi. 2010. Serpulidae (Annelida, Polychaeta) from Patton-Murray Seamounts, Gulf of Alaska, North Pacific Ocean. *Zootaxa* **2665:** 51–68.

Kupriyanova, E. K., and G. W. Rouse. 2008. Yet another example of paraphyly in Annelida: molecular evidence that Sabellidae contains Serpulidae. *Mol. Phylogenet. Evol.* **46:** 1174–1181.

Kupriyanova, E. K., Y. Sun, H. A. ten Hove, E. Wong, and G. W. Rouse. 2015. Serpulidae (Annelida) of Lizard Island, Great Barrier Reef, Australia. *Zootaxa* **4019:** 275–353.

Langmead, B., and S. L. Salzberg. 2012. Fast gapped-read alignment with Bowtie 2. *Nat. Methods* **9:** 357–359.

Lawrence, P. A., and F. B. Krasne. 1965. Annelid ciliary photoreceptors. *Science* **148:** 965–966.

Lehrke, J., H. A. ten Hove, T. A. Macdonald, T. Bartolomaeus, and C. Bleidorn. 2007. Phylogenetic relationships of Serpulidae (Annelida: Polychaeta) based on 18S rDNA sequence data, and implications for opercular evolution. *Org. Divers. Evol.* **7:** 195–206.

Leutscher-Hazelhoff, J. T. 1984. Ciliary cells evolved for vision hyperpolarize—Why? *Naturwissenschaften* **71:** 213–214.

Li, L., M. J. Connors, M. Kolle, G. T. England, D. I. Speiser, X. Xiao, J. Aizenberg, and C. Ortiz. 2015. Multifunctionality of chiton biomineralized armor with an integrated visual system. *Science* **350:** 952–956.

Mak, P. M. S. 1982. The coral associated polychaetes of Hong Kong, with special reference to the serpulids. Pp. 596–617 in *Proceedings of the first International Marine Biology Workshop: The Marine Flora and Fauna of Hong Kong and Southern China*, B. S. Morton and C. K. Tseng, eds. Hong Kong University Press, Hong Kong.

Miller, M. A., W. Pfeiffer, and T. Schwartz. 2010. Creating the CIPRES Science Gateway for inference of large phylogenetic trees. 2010 Gateway Computing Environments Workshop (GCE), New Orleans, LA. [Online]. IEEE Xplore Digital Library. Available: http://ieeexplore.ieee.org/document/5676129/ [2017, September 26].

Monro, C. C. A. 1933. The Polychaeta Sedentaria collected by Dr. C. Crossland at Colón in the Panama region and the Galapagos Islands during the expedition of the S.Y. St. George. *Proc. Zool. Soc. Lond.* **2:** 1039–1092.

Montagu, G. 1803. *Testacea Britannica or Natural History of British Shells, Marine, Land, and Fresh-Water, Including the Most Minute: Systematically Arranged and Embellished with Figures*. J. White, London.

Montagu, G. 1813. Descriptions of several new or rare animals, principally marine, discovered on the south coast of Devonshire. *Trans. Linn. Soc. Lond.* **11:** 1–26.

Mörch, O. A. L. 1863. Revisio critica Serpulidarum. Et Bidrag til Rørormenes Naturhistorie. *Naturhistorisk Tidsskrift København* **1:** 347–470.

Nicol, J. A. C. 1948. The giant axons of annelids. *Q. Rev. Biol.* **23:** 291–323.

Nicol, J. A. C. 1950. Responses of *Branchiomma vesiculosum* (Montagu) to photic stimulation. *J. Mar. Biol. Assoc. UK* **29:** 303–320.

Nilsson, D.-E. 1994. Eyes as optical alarm systems in fan worms and ark clams. *Philos. Trans. R. Soc. Biol. Sci. B* **346:** 195–212.

Nilsson, D.-E. 2009. The evolution of eyes and visually guided behaviour. *Philos. Trans. R. Soc. Biol. Sci. B* **364:** 2833–2847.

Nilsson, D.-E. 2013. Eye evolution and its functional basis. *Vis. Neurosci.* **30:** 5–20.

Orrhage, L. 1980. On the structure and homologues of the anterior end of the polychaete families Sabellidae and Serpulidae. *Zoomorphology* **96:** 113–168.

Orrhage, L., and M. C. M. Müller. 2005. Morphology of the nervous system of Polychaeta (Annelida). *Hydrobiologia* **535:** 79–111.

Pallas, P. S. 1766. *Miscellanea zoologica: quibus novae imprimis atque obscurae animalium species describuntur et observationibus iconibusque illustrantur*. Petrum van Cleef, Hagae Comitum.

Pezner, A. K., A. R. Lim, J. J. Kang, T. C. Armenta, and D. T. Blumstein. 2017. Hiding behavior in Christmas tree worms on different time scales. *Behav. Ecol.* **28:** 154–163.

Pillai, T. G. 1971. Studies on a collection of marine and brackish-water polychaete annelids of the family Serpulidae from Ceylon. *Ceylon J. Sci. Biol. Sci.* **9:** 88–130.

Pixell, H. L. M. 1913. Polychaeta of the families Serpulidae and Sabellidae, collected by the Scottish National Antarctic Expedition. *Trans. R. Soc. Edinb.* **49:** 347–358.

Porter, M. L., J. R. Blasic, M. J. Bok, E. G. Cameron, T. Pringle, T. W. Cronin, and P. R. Robinson. 2012. Shedding new light on opsin evolution. *Proc. R. Soc. Lond. Biol. Sci. B* **279:** 3–14.

Prentiss, N. K., K. Vasileiadou, S. Faulwetter, C. Arvanitidis, and H. A. ten Hove. 2014. A new genus and species of Serpulidae (Annelida, Polychaeta, Sabellida) from the Caribbean Sea. *Zootaxa* **3900:** 204–222.

Purschke, G. 2005. Sense organs in polychaetes (Annelida). Pp. 53–78 in *Morphology, Molecules, Evolution and Phylogeny in Polychaeta and Related Taxa*, T. Bartolomaeus and G. Purschke, eds. Springer, Berlin.

Purschke, G., D. Arendt, H. Hausen, and M. C. M. Müller. 2006. Photoreceptor cells and eyes in Annelida. *Arthropod Struct. Dev.* **35:** 211–230.

Radl, E. 1912. *Neue Lehre vom Zentralen Nervensystem*. Engelmann, Leipzig.

Ramirez, M. D., A. N. Pairett, M. S. Pankey, J. M. Serb, D. I. Speiser, A. J. Swafford, and T. H. Oakley. 2016. The last common ancestor of most bilaterian animals possessed at least nine opsins. *Genome Biol. Evol.* **8:**3640–3652.

Reynolds, E. S. 1963. The use of lead citrate at high pH as an electron-opaque stain in electron microscopy. *J. Cell. Biol.***17:** 208–212.

Rioja, E. 1931. Estudio de los políquetos de la Península Ibérica. *Mem. R. Acad. Cienc.* **2:** 1–472.

Rullier, F. 1948. La vision et l'habitude chez *Mercierella enigmatica* Fauvel. *Bull. Lab. Marit. Dinard* **30:** 21–27.

Schmarda, L. K. 1861. *Neue Wirbellose Thiere: Beobachted und Gesammelt auf einer Reise um die Erdr 1853 bis 1857*, I, *Turbellarien, Rotatorien und Anneliden*. W. Engelmann, Leipzig.

Smith, R. C., and K. S. Baker. 1981. Optical properties of the clearest natural waters (200–800 nm). *Appl. Opt.* **20:** 177–184.

Smith, R. S. 1984a. Development and settling of *Spirobranchus giganteus* (Polychaeta: Serpulidae). Pp. 461–483 in *Proceedings of the First International Polychaete Conference*, P. A. Hutchings, ed. Linnean Society of New South Wales, Sydney.

Smith, R. S. 1984b. Novel organelle associations in photoreceptors of a serpulid polychaete worm. *Tissue Cell* **16:** 951–956.

Smith, R. S. 1985. Photoreceptors of serpulid polychaetes. Ph.D. dissertation, James Cook University, Townsville, Australia.

Speiser, D. I., and S. Johnsen. 2008a. Comparative morphology of the concave mirror eyes of scallops (Pectinoidea). *Am. Malacol. Bull.* **26:** 27–33.

Speiser, D. I., and S. Johnsen. 2008b. Scallops visually respond to the size and speed of virtual particles. *J. Exp. Biol.* **211:** 2066–2070.

Speiser, D. I., D. J. Eernisse, and S. Johnsen. 2011. A chiton uses aragonite lenses to form images. *Curr. Biol.* **21:** 665–670.

Speiser, D. I., M. S. Pankey, A. K. Zaharoff, B. A. Battelle, H. D. Bracken-Grissom, J. W. Breinholt, S. M. Bybee, T. W. Cronin, A. Garm, A. R. Lindgren *et al*. 2014. Using phylogenetically-informed annotation (PIA) to search for light-interacting genes in transcriptomes from non-model organisms. *BMC Bioinformatics* **15:** R114–R126.

Stamatakis, A. 2006. RAxML-VI-HPC: maximum likelihood-based phylogenetic analyses with thousands of taxa and mixed models. *Bioinformatics* **22:** 2688–2690.

Stavenga, D. G., R. P. Smits, and B. J. Hoenders. 1993. Simple exponential functions describing the absorbance bands of visual pigment spectra. *Vis. Res.* **33:** 1011–1017.

Straughan, D. 1967. Marine Serpulidae (Annelida: Polychaeta) of eastern Queensland and New South Wales. *Aust. J. Zool.* **15:** 201–261.

Su, C.-Y., D.-G. Luo, A. Terakita, Y. Shichida, H.-W. Liao, M. A. Kazmi, T. P. Sakmar, and K.-W. Yau. 2006. Parietal-eye phototransduction components and their potential evolutionary implications. *Science* **311:** 1617–1621.

ten Hove, H. A., and E. K. Kupriyanova. 2009. Taxonomy of Serpulidae (Annelida, Polychaeta): the state of affairs. *Zootaxa* **2036:** 1–126.

ten Hove, H. A., and F. J. A. Pantus. 1985. Distinguishing the genera *Apomatus* Philippi, 1844 and *Protula* Risso, 1826 (Polychaeta: Serpulidae): a further plea for a methodical approach to serpulid taxonomy. *Zool. Meded.* **59:** 419–437.

Tsukamoto, H., I. S. Chen, Y. Kubo, and Y. Furutani. 2017. A ciliary opsin in the brain of a marine annelid zooplankton is UV-sensitive and the sensitivity is tuned by a single amino acid residue. *J. Biol. Chem.* **292:** 12971–12980.

Uchida, H. 1978. Serpulid tube worms (Polychaeta, Sedentaria) from Japan with the systematic review of the group. *Bull. Mar. Park Res. Stn.* **2:** 1–98.

Ullrich-Lüter, E. M., S. Dupont, E. Arboleda, H. Hausen, and M. I. Arnone. 2011. Unique system of photoreceptors in sea urchin tube feet. *Proc. Natl. Acad. Sci. U.S.A.* **108:** 8367–8372.

Vine, P. J., and J. H. Bailey-Brock. 1984. Taxonomy and ecology of coral reef tube worms (Serpulidae, Spirorbidae) in the Sudanese Red Sea. *Zool. J. Linn. Soc.* **80:** 135–156.

Vöcking, O. 2016. The larval photoreceptors of the mollusk *Leptochiton asellus*. Ph.D. dissertation, University of Bergen, Norway.

Wald, G., and S. Rayport. 1977. Vision in annelid worms. *Science* **196:** 1434–1439.

WoRMS. 2017. World Register of Marine Species. [Online]. Available: http://www.marinespecies.org [2017, October 24].

Yerramilli, D., and S. Johnsen. 2010. Spatial vision in the purple sea urchin *Strongylocentrotus purpuratus* (Echinoidea). *J. Exp. Biol.* **213:** 249–255.

Zibrowius, H. 1969. Quelques nouvelles recoltes de Serpulidae (Polychaeta Sedentaria) dans le Golfe de Gabes et en Tripolitaine. Description de *Vermiliopsis pomatostegoides* n. sp. *Bull. Inst. Natl. Sci. Technol. Océanogr. Pêche* **1:** 123–137.

Appendix

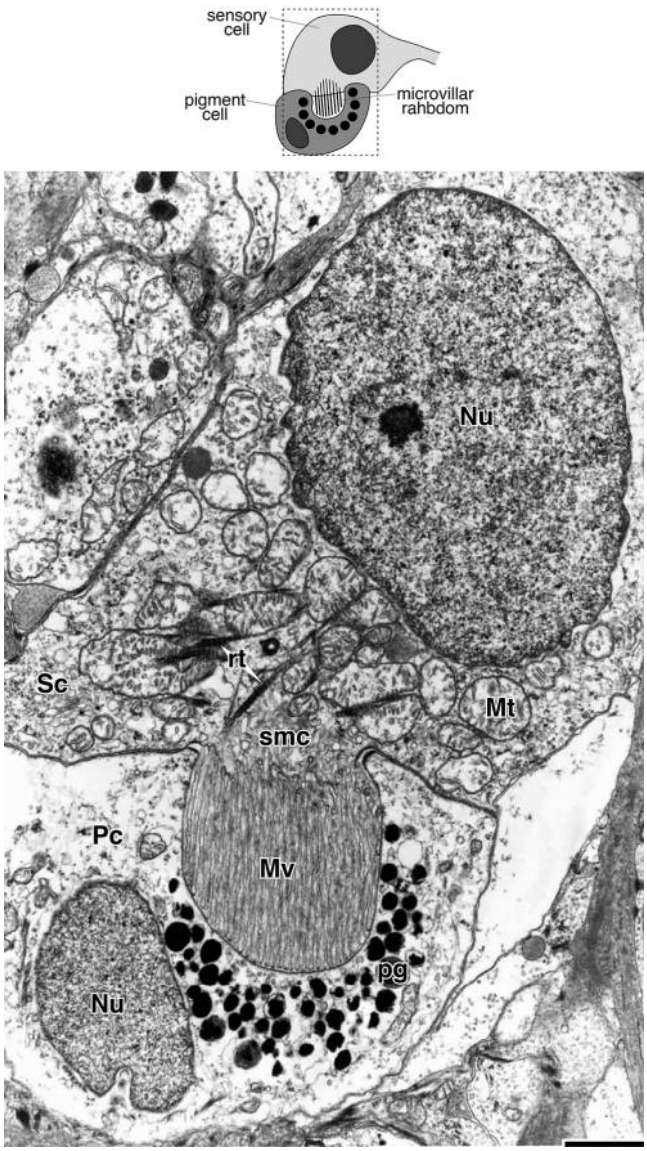

Figure A1. Transmission electron micrograph of a *Spirobranchus corniculatus* rhabdomeric cerebral ocellus. A simple diagram of the structure is shown above, with a dashed box representing the micrograph frame. Mv, microvilli; Mt; mitochondrion; Nu, nucleus; Pc, pigment cell; pg, pigment granules; rt, rootlets; Sc, sensory cell; smc, submicrovillar cisternae. Scale bar = 1 μm.

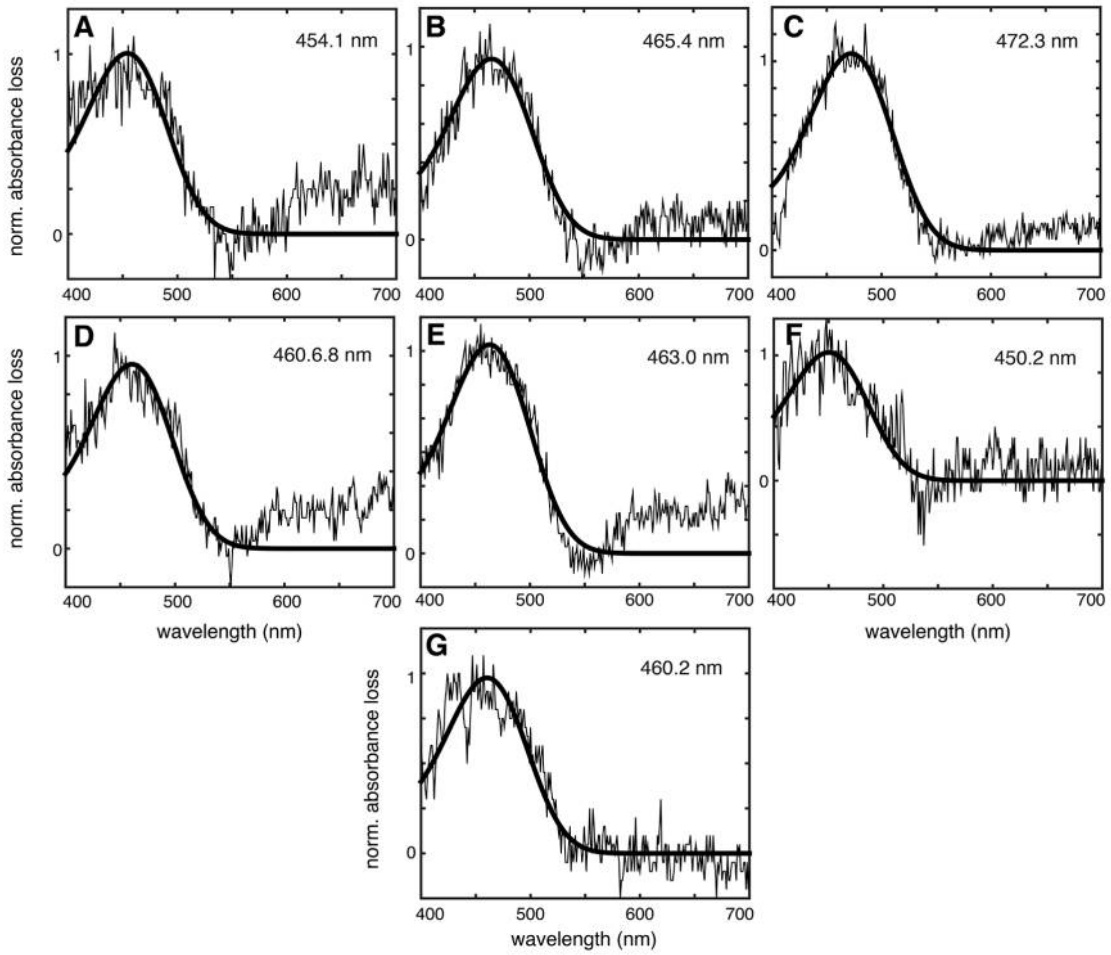

Figure A2. *Spirobranchus corniculatus* visual pigments. Individual normalized and baselined pre- and post-bleach microspectrophotometry difference spectra of *S. corniculatus* radiolar eye ocellar visual pigments. Plotted are raw difference spectra (thin lines) and their best-fit visual pigment template (thick lines) (Stavenga *et al.*, 1993). The visual pigment wavelength of maximum absorbance (λ_{max}) is indicated on each plot.

Table A1

Phototransduction and eye development transcripts found in Spirobranchus corniculatus *radiolar eyes*

Gene	*Spirobranchus* contig	Length (AA)	Expression level (FPKM)
Phototransduction			
c-opsin	Contig8581	89	26.1
	Contig4115	140	34.7
	Contig3572	375	57.7
$G\alpha_o$ subunit	Contig2631	314	35.7
$G\alpha_s$ subunit	Contig7033	399	24.2
$G\alpha_i$ subunit	Contig2262	332	61.2
	Contig1627	360	90.0
G-protein β subunit	Contig1743	348	84.9
gngt1C	Contig1156	94	193.0
	Contig5969	68	68.5
PKC	Contig8162	126	22.1
	Contig5155	665	21.4
	Contig2135	490	44.0
cnga1	Contig5735	490	26.2
RGS9	Contig8113	164	45.7
	Contig3307	134	47.0
	Contig2832	261	54.0
	Contig2325	261	58.2
	Contig2237	255	59.0
rdgB	Contig2509	213	47.4
arr	Contig 7055	430	17.1
GC	Contig6184	505	26.4
	Contig3010	265	43.8
PDE6abc	Contig6368	405	20.9
Eye development			
eya	Contig7479	347	24.8
	Contig4021	367	32.6
six4	Contig1089	379	88.7
so	Contig3211	193	60.3
	Contig2044	363	57.2
pax6	Contig7351	463	22.9
glass	Contig6982	316	17.6
dpp	Contig5984	370	24.2
Other light sensing			
cry	Contig5137	337	20.5
	Contig7592	258	19.8

The *de novo* assembly (and raw transcriptomic sequence reads) used for phylogenetically informed annotation (PIA) identification of phototransduction contigs are available at the National Center for Biotechnology Information Sequence Read Archive under bioproject PRJNA399760, biosample SAMN07949790. FPKM, fragments per kilobase million.